American Journal of Astronomy and Astrophysics
2024, Vol. 11, No. 3, pp. 74-91
https://doi.org/10.11648/j.ajaa.20241103.12

Research Article

Unravelling the Enigmatic Nexus: Black Holes, Dark Matter, and the Interplay of Light, Gravity, and Electromagnetic Forces in Astrophysics and Astronomy

Wim Vegt*

Department of Physics, Eindhoven University of Technology, Eindhoven, The Netherlands

Abstract

This research introduces a mathematical model positioning our physical reality within a ten-dimensional hyperspace, in which time acts as the unifying coordinate linking three-dimensional electric, magnetic, and gravitational spaces. Each domain is characterized by its respective field—electric, magnetic, or gravitational—and governed by intrinsic divergences and rotations, leading to a universal property known as Force Density, expressed in [N/m ³]. This Force Density facilitates interactions among the distinct spaces while adhering to the principle of equilibrium, which posits that cumulative force densities from disturbances must consistently sum to zero. Building upon Einstein's General Relativity—which describes the curvature of spacetime by gravitational fields and assumes a constant light speed—this study proposes a perspective wherein light speed may vary during coherent laser beam interactions, prompting a re-examination of gravitational and luminous interactions across scales. The proposed model integrates the Stress-Energy Tensor and Gravitational Tensor, introducing a new tensor representation for black holes, termed Gravitational Electromagnetic Confinements, incorporating electromagnetic energy gradients and Lorentz transformations. This framework transcends traditional General Relativity, particularly evident in gravitational lensing. By reinterpreting Einstein's incorporation of the Gravitational Constant within the Energy-Stress Tensor, this work harmonizes gravity and light, offering insights into black hole solutions resonating with John Archibald Wheeler's 1955 research. Empirical data from Galileo satellites and MASER frequency measurements underscore discrepancies between established theories and this new model, enhancing the precision of gravitational observations. Through the confluence of Quantum Physics and General Relativity, as seen in approaches like String Theory, this interdisciplinary endeavor revisits the gravitational constant "G," redefining it while bridging theoretical frameworks, thus paving the way for breakthroughs in astronomical and astrophysical sciences.

Keywords

Black Holes, Dark Matter, General Relativity, Gravitational Redshift, Gravitational Electromagnetic Interaction, Gravitational Lensing, Quantum Physics, String Theory

*Corresponding author: wimvegt@quantumlight.science (Wim Vegt)

Received: 13 July 2024; **Accepted:** 10 September 2024; **Published:** 10 October 2024

1. Gravity

1.1. Introduction

This scholarly work introduces an innovative paradigm concerning the essence of gravity, positing it as an inherent property of a ten-dimensional spatial construct. Within this paradigm, gravitational fields are interpreted as emergent attributes resulting from a three-dimensional projection, akin to the manifestation of electric and magnetic fields within separate projections of the same ten-dimensional continuum. The tenth dimension is exclusively designated for the temporal axis, serving as the cohesive dimension that unifies the nine spatial dimensions, thereby forming the palpable three-dimensional physical reality that is experienced.

The interaction of analogous fields engenders an effect within our physical realm, manifested as a force density, which is quantified in units of [N/m^3]. Specifically, the convergence of two superimposed gravitational fields results in a gravitational force density. Similarly, the interplay of two overlapping electric fields gives rise to an electric force density, whereas the intersection of overlapping magnetic fields culminates in a magnetic force density. Through the integration of these force densities across the entire volume, the total interaction force can be deduced.

For instance, when an individual stands on a scale, the scale measures the total interaction force. This force is calculated by integrating, over an infinite volume, all gravitational interaction force densities arising from the interplay between the individual's entire gravitational field and the Earth's gravitational field. Force densities are interchangeable: hence, the overall interaction forces density results from the summation of electric, magnetic, and gravitational force densities. Consequently, light interacts with a gravitational field, as elucidated in equation (6). The Lorentz transformations describe the conversion between the three-dimensional electric domain and the three-dimensional magnetic domain, and vice versa, dependent on the relative velocity between the observer and the respective field. Analogously, a similar transformation is expected to occur within gravitational fields as a consequence of accelerations. Vegt Wim (26-Oct-2022) [14].

1.2. A New Paradigm for Gravity

Einstein approached the interaction between gravity and light by the introduction of the “Einstein Gravitational Constant” in the 4-dimensional Energy-Stress Tensor.

$$G_{\mu\nu} + \Lambda\, g_{\mu\nu} = \kappa\, T_{\mu\nu} \tag{1}$$

In which $G_{\mu\nu}$ equals the Einstein Tensor, $g_{\mu\nu}$ equals the Metric Tensor, $T_{\mu\nu}$ equals the Stress-Energy tensor, Λ equals the cosmological constant and κ equals the Einstein gravitational constant.

The core principle underlying General Relativity pertains to a curved 4-dimensional Space-Time Continuum. Similarly, the fundamental concept in this novel theory revolves around a 4-dimensional Universal Equilibrium delineated by equation (6).

Central to this novel theory is the vectorial summation of force densities denoted in [N/m^3]. Force densities hold universal significance and are interchangeable irrespective of their source. Vegt Wim (1995) [10] Within this framework, fields solely engage with analogous fields. The theory contemplates three distinct categories of physical fields: Electric Fields, Magnetic Fields, and Gravitational Fields.

The outcome of the interaction between two corresponding fields manifests as a force density articulated in [N/m^3]. When two electric fields interact, the resultant force density is an electric force density delineated in [N/m^3]. Similarly, the convergence of two magnetic fields yields a magnetic force density expressed in [N/m^3]. Likewise, the intersection of two gravitational fields produces a gravitational force density expressed in [N/m^3]. At the core of this theory lies the foundational principle that all force densities collectively establish a universal equilibrium. This elucidation can be found in Reference [13], specifically detailed within equations (4) through (22).

The vectorial force densities are derived from the divergence of the sum of the Electromagnetic Stress-Energy tensor $\overline{\overline{T}}$ and a selected Gravitational Tensor $\overline{\overline{J}}$.

$$\kappa\, T_{\mu\nu} \Leftrightarrow T_{\mu\nu} + J_{\mu\nu} \tag{2}$$

The 4-dimensional divergence of the sum of the Electromagnetic Stress-Energy tensor and the Gravitational Tensor expresses the 4-dimensional Force-Density vector (expressed in [N/m^3] in the 3 spatial coordinates) as the result of Electro-Magnetic-Gravitational interaction.

$$f^{\mu} = \partial_{\nu} \left(T^{\mu\nu} + J^{\mu\nu} \right) \tag{3}$$

In vector notation the 4-dimensional Force-Density vector can be written as:

$$\overline{f}^{4} = \begin{pmatrix} f_4 \\ f_3 \\ f_2 \\ f_1 \end{pmatrix} = \square \bullet \left(\overline{\overline{T}} + \overline{\overline{J}} \right) \tag{4}$$

The fundamental boundary condition for this alternative approach to gravity is the requirement that the Force 4 vector equals zero in the 4 dimensions, expressing a universal 4-dimensional equilibrium Vegt Wim (1995) [10]:

$$\bar{f}^4 = \begin{pmatrix} f_4 \\ f_3 \\ f_2 \\ f_1 \end{pmatrix} = \square \bullet \left(\bar{\bar{T}} + \bar{\bar{J}} \right) = \bar{0}^4 \qquad (5)$$

Within this innovative framework, the interactions among electric-electric fields, magnetic-magnetic fields, and gravitational-gravitational fields are interchangeable. Consequently, the gravitational force density mirrors a comparable structure to that of the electric force density and the magnetic force density. The three spatial components of the Force-Density vector arising from the Electro-Magnetic-Gravitational interaction can be expressed as:

$$\bar{f} = -\frac{1}{c^2}\frac{\partial (\bar{E} \times \bar{H})}{\partial t} + \varepsilon_0 \bar{E} (\nabla . \bar{E}) - \varepsilon_0 \bar{E} \times (\nabla \times \bar{E}) +$$

$$+ \mu_0 \bar{H} (\nabla . \bar{H}) - \mu_0 \bar{H} \times (\nabla \times \bar{H}) + \gamma_0 \bar{g} (\nabla . \bar{g}) - \gamma_0 \bar{g} \times (\nabla \times \bar{g}) = \bar{0} \quad [N/m^3]$$

in which:

$\varepsilon_0 (\nabla . \bar{E}) = \rho_E$ Electric Charge Density [C/ m^3]

$\mu_0 (\nabla . \bar{H}) = \rho_M$ Magnetic Flux Density [Vs/ m^3] or [Wb/ m^3] (6)

$\gamma_0 (\nabla . \bar{g}) = \rho_M$ Mass Density (Electromagnetic) [kg/ m^3]

Electric Energy Density: $w_E = \frac{1}{2} \varepsilon_0 E^2$

Magnetic Energy Density: $w_M = \frac{1}{2} \mu_0 H^2$

Gravitational Energy Density: $w_G = \frac{1}{2} \gamma_0 g^2$

In which E represents the electric field intensity expressed in [V/m], H represents the magnetic field intensity expressed in [A/m] and g represents the gravitational acceleration expressed in [m/s^2]. The permittivity indicated as, ε_0 the permeability indicated as μ_0 and the gravitational permeability of vacuum as γ_0. Vegt Wim (2002) [11] and Vegt Wim (26-Oct-2022) [14].

The initial term in equation (6) portrays the inertia inherent in electromagnetic radiation, while the succeeding terms, two and three, denote the interaction between electric fields. Subsequently, the fourth and fifth terms represent the interaction of magnetic fields, and the sixth and seventh terms pertain to gravitational field interactions.

At the heart of this newly suggested theory resides a fundamental notion of universal equilibrium, demonstrating a pervasive presence across temporal, directional, and spatial dimensions. This overarching equilibrium finds concise representation through the zero-vector placed on the right-hand side of the equality symbol. An instance illustrating three-dimensional universal equilibrium is akin to the projection of a slide onto a screen [4].

In the realm of curl-free gravitational fields [25, 29], equation (6) is identical to equation (22) delineated in References [11, 25]. In the context of curl-free gravitational fields Weng Zihua, (October 2008) [25, 29], equation (6) may be reformulated as follows:

$$\bar{f} = -\frac{1}{c^2}\frac{\partial (\bar{E} \times \bar{H})}{\partial t} + \varepsilon_0 \bar{E} (\nabla . \bar{E}) - \varepsilon_0 \bar{E} \times (\nabla \times \bar{E}) + \\ + \mu_0 \bar{H} (\nabla . \bar{H}) - \mu_0 \bar{H} \times (\nabla \times \bar{H}) + \bar{g} \rho_M = \bar{0} \quad [N/m^3] \qquad (7)$$

Substituting Einstein's W = m c^2 in (7) results in "Electro-Magnetic-Gravitational Equilibrium Field Equation" (8) Vegt Wim (2 Oct, 2021) [12], Vegt Wim (14 October 2022) [13] and Vegt Wim (26-Oct-2022) [14]:

$$\bar{f} = -\frac{1}{c^2}\frac{\partial (\bar{E} \times \bar{H})}{\partial t} + \varepsilon_0 \bar{E} (\nabla . \bar{E}) - \varepsilon_0 \bar{E} \times (\nabla \times \bar{E}) + \mu_0 \bar{H} (\nabla . \bar{H}) \\ - \mu_0 \bar{H} \times (\nabla \times \bar{H}) + \frac{1}{2c^2} \bar{g} \left(\varepsilon E^2 + \mu H^2 \right) = \bar{0} \quad [N/m^3] \qquad (8)$$

The theory describes “Electromagnetic-Gravitational Interaction”, “Magnetic-Gravitational Interaction” and “Electric-Gravitational Interaction”. In this new theory particles do not interact with fields. The interaction between an electric charged particle and an electric field is not the interaction between a particle and a field but it is the interaction between the electric field of the particle interacting with the other electric field. Every interaction is an interaction between fields. Electric Fields interact with Electric Fields, Magnetic Fields interact with Magnetic Fields and Gravitational Fields only interact with Gravitational Fields. Raymond J. Beach (2014) [8].

The consequence thereof is the dissemination of light (Electromagnetic Radiation) at the precise velocity of light ascertained by an Electro-Magnetic Perfect Equilibrium in all directions, at any given point, and at any temporal juncture.

Vegt Wim (Calculation 1, June 21, 2022) [15] posited this notion. This principle stands in opposition to Maxwell's theory of Electrodynamics, within which the speed of light is exclusively applicable to planar electromagnetic waves. Maxwell James Clerk (01 January 1865) [6]. The concept of the Universal Perfect Equilibrium transcends such limitations, applying to all manifestations of light, ranging from Laser Beams to the imagery depicting the genesis of the Universe.

2. “Gravitational RedShift/BlueShift in “Light (EMR)” Due to Electromagnetic Gravitational Interaction”

To validate the New Theory, the experiment titled "Test of the Gravitational Redshift with Galileo Satellites in an Eccentric Orbit" was selected. Herrmann Sven, Felix Finke, Martin Lülf, Olga et al. (4 December 2018) [8] In this experiment, a stable MASER frequency from a ground station was transmitted to two Galileo Satellites. The frequency difference between the Ground Station and the Satellites was measured. This frequency shift was due to the gravitational field of the Earth, and two satellites were chosen to account for the eccentricity of the Galileo orbit.

Gravitational fields influence the propagation of electromagnetic radiation, specifically causing a phenomenon known as gravitational redshift. According to General Relativity, light or any form of electromagnetic radiation loses energy when it escapes a gravitational field, leading to an increase in wavelength and a corresponding decrease in frequency. In the "Test of the Gravitational Redshift" experiment, the MASER signal experiences this effect as it travels from the ground station (lower gravitational potential) to the satellites (higher gravitational potential). The difference in frequency recorded by the satellites is a direct measure of this redshift. By carefully selecting two satellites in slightly different orbits, the experiment compensates for the orbit's eccentricity, ensuring more precise measurements of the gravitational redshift. This effect highlights the interplay between gravity and electromagnetic radiation Vegt Wim (Calculation 3, August 25, 2022) [17], confirming theoretical predictions with practical observations.

Assuming a gravitational field g[z] depending on the radial direction in cartesian coordinates between the ground station and the satellites:

$$\overline{g[z]} = \left\{0,0,\ \frac{G\ M_{Earth}}{4\ \pi\ z^2}\right\} \tag{9}$$

In which G (G = 6.67428 10^{-11} Nm^2/kg^2) equals the Gravitational constant, M_{Earth} the mass of the earth and r the radial distance from the centre of the earth. The mathematical solution [5] of equation (8) for plane electromagnetic waves (expressed in cartesian {x,y,z} coordinates) related to the Electric Field Intensity equals:

$$\overline{E} = \begin{pmatrix} E_x \\ E_y \\ E_z \end{pmatrix} = \begin{pmatrix} e^{-\frac{G\ M_{Eearth}\ \varepsilon_0\ \mu_0}{8\ \pi\ z}}\ h\left[\ \omega_0\ e^{-\frac{G\ M_{Earth}\ \varepsilon_0\ \mu_0}{4\ \pi\ z}}\left(t - \sqrt{\varepsilon\ \mu}\ z\right)\right] \\ 0 \\ 0 \end{pmatrix} \tag{10}$$

And the mathematical solution of (8) for the Magnetic Field Intensity equals:

$$\overline{H} = \begin{pmatrix} H_x \\ H_y \\ H_z \end{pmatrix} = \begin{pmatrix} 0 \\ \frac{1}{\sqrt{\varepsilon_0\ \mu_0}}\ e^{-\frac{G\ M_{Earth}\ \varepsilon_0\ \mu_0}{8\ \pi\ z}}\ h\left[\ \omega_0\ e^{-\frac{G\ M_{Earth}\ \varepsilon_0\ \mu_0}{4\ \pi\ z}}\left(t - \sqrt{\varepsilon\ \mu}\ z\right)\right] \\ 0 \end{pmatrix} \tag{11}$$

In this scenario, the initial frequency of the MASER radiation propagating in the direction of the Earth's gravitational field g[z] is denoted by ω_0. The inclusion of the exponential term indicates the Gravitational Redshift encountered as the MASER radiation traverses the Earth's gravitational field. While the speed of propagation of Electromagnetic Radiation (i.e., the speed of light) stays consistent, both the amplitude of the field intensity and the frequency undergo an exponential decline..

Mathematical calculations compare the results obtained from General Relativity with those from the New Theory. By setting the distance from the ground station to the Earth's centre as z_1 = 6,378,000 [m] (Earth's radius) and the average distance of ESA satellites in a Galileo orbit as z_2 = 23,222,000 [m] (distance from the ESA satellite to the Earth's centre), the Gravitational Redshift, Delva P, Puchades N, Schönemann E, Dilssner F, Courde C et all (December 2018) [2] and Herrmann Sven, Felix Finke, Martin Lülf, Olga, et all (December 2018) [5], As per the principles established in General Relativity, this value is ascertained Vegt Wim (Calculation 2, July 16, 2023) [16]:

$$\Delta\,\omega_{GR} = 0.00000000004011815497097883\ [s^{-1}] \quad (12)$$

Calculated with Mathematica, the Gravitational RedShift [2, 5, 6, 17] according the New Theory, which is a solution of equation (8) equals Vegt Wim (Calculation 2, July 16, 2023) [16]:

$$\Delta\,\omega_{GR} = 0.00000000004011824206173742\ [s^{-1}] \quad (13)$$

Both calculated values a within the Range of the measured gravitational RedShift by the average values of both ESA satellites in the Galileo orbit.

$$\Delta\,\omega_{Measured} = 0.000000000040118 \pm 2.2\,10^{-15}\ [s^{-1}] \quad (14)$$

In [2] a factor α has been defined which presents the measured deviation α between the predicted Gravitational RedShift by General Relativity and the Measured Gravitational RedShift.

$$\alpha = \Delta\,\omega_{MEASURED} - \Delta\,\omega_{GR} = (2.2 \pm 1.6) \times 10^{-5} \quad (15)$$

A comparable factor α can be used to determine which theory (General Relativity or the New Theory) has the nearest approach to the experimentally measured data. Highly accurate measuring experiments are required with an accuracy higher than 16 digits beyond the decimal point.

3. Black Holes Without Singularities with Dimensions Smaller Than the Diameter of the Hydrogen Atom

A second fundamental solution for equation (8) describes a Gravitational Electromagnetic Confinement (BLACK HOLE) [1] within a radial gravitational field with acceleration $\bar{g}$ (in radial direction). This solution represents a Black Hole, the confinement of light due to its own gravitational field, and has no singularities. This solution for equation (8) describes Black Holes, dependent of time and radius, presenting discrete spherical energy levels, within a radial gravitational field with acceleration $\bar{g}$ (in radial direction) has been represented in (16) and (17).

$$\begin{pmatrix} E_r \\ E_\theta \\ E_\varphi \end{pmatrix} = \begin{pmatrix} 0 \\ f(r)\,\mathrm{Sin}(k\,r)\,\mathrm{Sin}(\omega\,t) \\ -f(r)\,\mathrm{Cos}(k\,r)\,\mathrm{Cos}(\omega\,t) \end{pmatrix} \quad \begin{pmatrix} H_r \\ H_\theta \\ H_\varphi \end{pmatrix} = \sqrt{\frac{\varepsilon}{\mu}} \begin{pmatrix} 0 \\ -f(r)\,\mathrm{Sin}(k\,r)\,\mathrm{Cos}(\omega\,t) \\ -f(r)\,\mathrm{Cos}(k\,r)\,\mathrm{Sin}(\omega\,t) \end{pmatrix} \quad \bar{g} = \begin{pmatrix} \frac{G_1}{4\,\pi\,r^2} \\ 0 \\ 0 \end{pmatrix}$$

$$w_{em} = \left(\frac{\mu_0}{2}\left(\bar{m}\,.\,\bar{m}\right) + \frac{\varepsilon_0}{2}\left(\bar{e}\,.\,\bar{e}\right)\right) = f(r)^2\left(\left(\mathrm{Sin}(k\,r)\,\mathrm{Sin}(\omega\,t)\right)^2 + \left(\mathrm{Cos}(k\,r)\,\mathrm{Cos}(\omega\,t)\right)^2 + \frac{\varepsilon}{\mu}\left(\mathrm{Sin}(k\,r)\,\mathrm{Cos}(\omega\,t)\right)^2 + \left(\mathrm{Cos}(k\,r)\,\mathrm{Sin}(\omega\,t)\right)^2\right) \quad (16)$$

In which the radial function f(r) equals:

$$f[r] = K\,e^{-\frac{G\,M_{BH}\,\varepsilon_0\,\mu_0}{8\,\pi\,r}} \quad (17)$$

G represents the Gravitational constant and M represents the total confined electromagnetic mass of the BLACK HOLE. Equation (16) presents a Standing (Confined) Electromagnetic Field Configuration with a phase shift of 90 degrees between the electric field and the magnetic field with the corresponding Nodes and AntiNodes. [11] The solution has been calculated according Newton's Shell Theorem. [23]

Assuming a constant speed of light "c" and Planck's constant ħ within the BLACK HOLE, the radius "R" (with n = 1, 2, 3, 4….) of the BLACK HOLE with the energy of a proton,

according $W = m_{proton}\, c^2$, would be: $1.5009211 \times 10^{-10}$ [J].

$$R_{GEON} = n\,\lambda = n\left(\frac{c}{f}\right) = n\left(\frac{c}{W}\right)\hbar = 7.1865\ 10^{-26}\left(\frac{n}{W}\right) \tag{18}$$

$$R_{GEON} = n\ 3.82\ 10^{-12}\ [m]$$

Black Holes (GEONs) Wheeler John Archibald (15 January 1955) [26] are varying from atomic dimensions with dimensions of 10^{-27} [kg], until Black Holes with dimensions of 10^{40} [kg], At these dimensions Black Holes turn into Dark Matter. The fundamental boundary condition for the confinement of Electromagnetic radiation (BLACK HOLEs) is that the energy flow (Poynting vector) $\bar{S} = \bar{E} \times \bar{H}$ equals zero at the surcface of the confinement. This is possible at every *"90 degrees Phase Shift Surface"* (*Sphere*) between the Electric Field and the Magnetic Field. [27, 28]

3.1. Black Holes with a Singular Point and Large Dimensions

Figure 1 represents a Black Hole (GEON) Wheeler John Archibald (15 January 1955) [26] with a mass of 10^{35} [kg] and a radius of about 25 [km] controlled by a different mahgematical solution for equation (8). The radius of the Black Hole equals about 25 [km] which has been controlled by a different mathematical solution (19) for equation (8).

$$f[r] = K\, e^{\left(\frac{G\, M_{BH}\, \varepsilon_0\, \mu_0}{8\,\pi\, r} - \log[r]\right)} \quad [J/m^3] \tag{19}$$

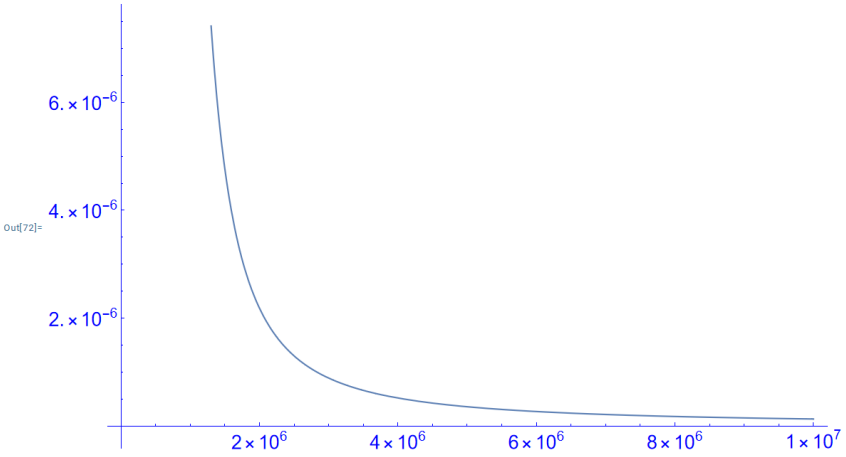

Figure 1. *The Energy Density [J/m³] as a function of the Radius R = max 10^7 [m] of the Black Hole.*

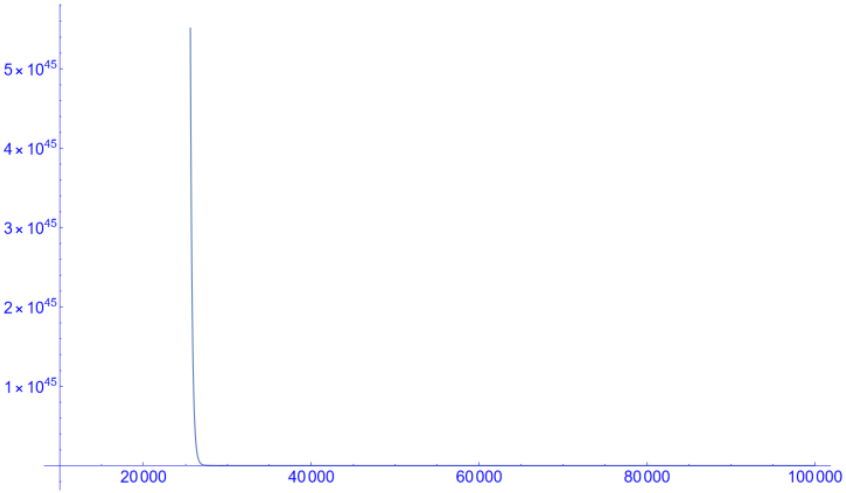

Figure 2. *The Energy Density [J/m³] as a function of the Radius R = max 10^5 [m].*

Figure 1 and Figure 2 Vegt Wim (Calculation 4 21 February 2023) [18] demonstrate the large effect of "Gravitational Intensity Shift" and "Gravitational RedShift" at the distance of 25 [km]. Over a distance of 10.000 [km] the intensity of the emitted light of the Black Hole with a mass of 10^{35} [kg] falls back with a factor of 10^{-51}. Also the frequency of the emitted light of the Black Hole falls back with a factor 10^{-51}. Emitted light in the visible spectrum of 10^{14} [Hz] falls back to a frequency of 10^{-37} [Hz]. These extreme low frequencies with extreme low intensities have never been measured which has result in the name "Black Hole" for the phenomenon of "Gravitational Intensity Shift" and "Gravitational RedShift" for a large mass. It follows from equation (8) and the solutions (10) and (11) that the speed of light does not change inside and around Black Hole. Only the direction of the propagation of light can change due to a gravitational field. Nikko John Leo S. Lobos, Reggie C. Pantig (2022). [7]

3.2. Dark Matter in the Universe Controlled by "Gravitational Shielding"

Figure 3 represents Dark Matter with a total mass of 10^{53} [kg] and a radius of about 10 times the size of the Milky Way Galaxy. The radius [11] of the dark mass equals 5 10^{21} [m] which has been controlled by a different mathematical solution (20) for equation (8).

$$f[r] = K\, e^{\left(\frac{G\, M_{BH}\, \varepsilon_0\, \mu_0}{8\, \pi\, r} - \log[r]\right)} \quad [J/m^3] \tag{20}$$

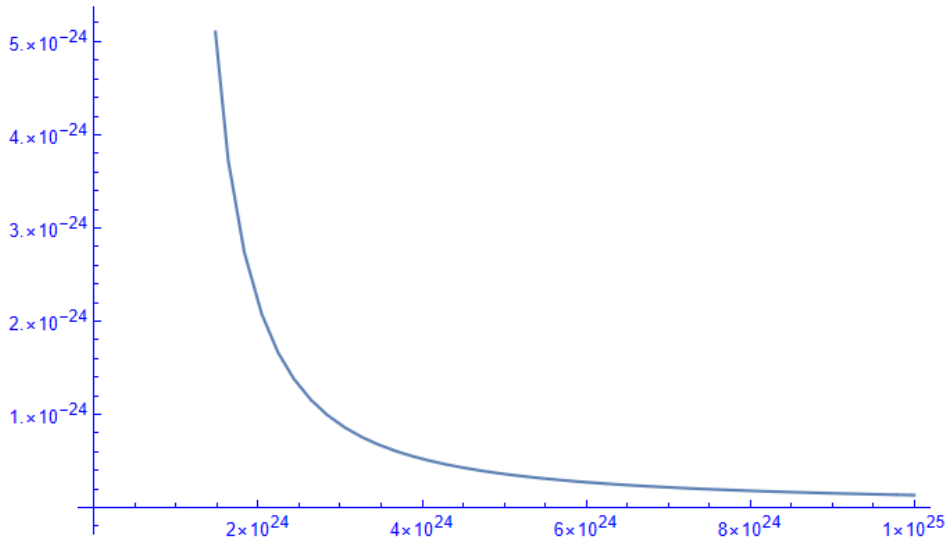

Figure 3. *The Energy Density [J/m^3] as a function of the Radius R = max 10^{25} [m] of the Dark Matter.*

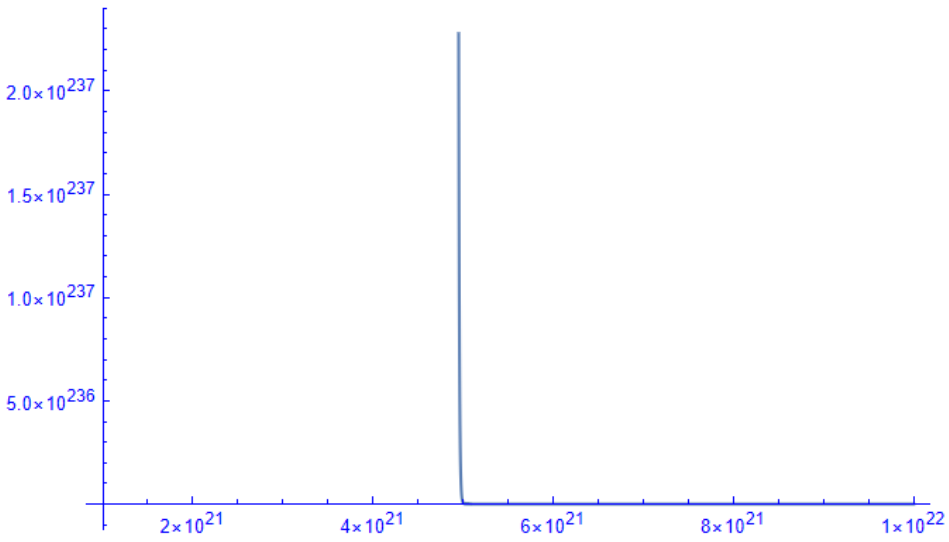

Figure 4. *The Energy Density [J/m^3] of the Dark Matter as a function of the Radius R = max 10^{22} [m].*

Figure 3 and Figure 4 demonstrate the large effect of "Gravitational Intensity Shift" and "Gravitational RedShift" at the distance of 5 10^{21} [m] which is 10 times the radius of the Milky Way Galaxy. Over the distance of 5 10^{21} [m] the intensity of the emitted light of the Dark Matter with a mass of 10^{53} [kg] falls back with a factor of 10^{-261}. Also the frequency of the emitted light of the Black Hole falls back with a factor 10^{-261}. Emitted light in the visible spectrum of 10^{14} [Hz] falls back to a frequency of 10^{-247} [Hz]. These extreme low frequencies with extreme low intensities have never been measured which has result in the name "Dark Matter" for the phenomenon of "Gravitational Intensity Shift" and "Gravitational RedShift" for an extreme large mass. It follows from equation (8) and the solutions (10) and (11) that the speed of light does not change inside and around the Dark Mass. Only the direction of the propagation of light can change due to the gravitational field of the Dark Mass.

4. The Relationship Between Black Holes and Quantum Physics

Introducing the Quantum Vector Function $\bar{\phi}$,

$$\bar{\phi} = \sqrt{\frac{\mu}{2}} \left(\bar{H} + i \frac{\bar{E}}{c} \right) \tag{21}$$

Substituting (21) in (16) results in the quantum presentation for the BLACK HOLE:

$$\overline{\Phi(r,\theta,\varphi)} = \sqrt{\frac{\mu}{2}} \left(\bar{H} + i \frac{\bar{E}}{c} \right) f(r) \begin{pmatrix} \Phi_r \\ \Phi_\theta \\ \Phi_\varphi \end{pmatrix}$$

$$\overline{\Phi(r,\theta,\varphi)} = K \sqrt{\frac{\varepsilon}{\mu}}\, e^{-\frac{G1\, \varepsilon_0\, \mu_0}{8\,\pi\, r}} \begin{pmatrix} 0 & 0 & 0 \\ 0 & -\mathrm{Sin}(k\,r) & \mathrm{Sin}(k\,r) \\ 0 & -i\,\mathrm{Cos}(k\,r) & i\,\mathrm{Cos}(k\,r) \end{pmatrix} \begin{Bmatrix} 0 \\ \mathrm{Cos}\,(\omega\, t) \\ i\,\mathrm{Sin}\,(\omega\, t) \end{Bmatrix} \tag{22}$$

With "K" a constant value dependend of the mass of the BLACK HOLE. The Dot product between the unit vector and the Quantum Vector Function $\bar{\phi}$ represents the quantum mechanical probability function $\Psi[r,t]$ which is a fundamental solution of the Schrödinger Wave Equation [12].

$$\overline{\Phi(r,\theta,\varphi)} = K \sqrt{\frac{\varepsilon}{\mu}}\, e^{-\frac{G1\, \varepsilon_0\, \mu_0}{8\,\pi\, r}} \begin{pmatrix} 0 & 0 & 0 \\ 0 & -\mathrm{Sin}(k\,r) & \mathrm{Sin}(k\,r) \\ 0 & -i\,\mathrm{Cos}(k\,r) & i\,\mathrm{Cos}(k\,r) \end{pmatrix} \begin{Bmatrix} 0 \\ \mathrm{Cos}\,(\omega\, t) \\ i\,\mathrm{Sin}\,(\omega\, t) \end{Bmatrix}$$

$$\Psi(r,t) = \{1 \;\; 1 \;\; 1\} \begin{Bmatrix} 0 \\ \mathrm{Cos}\,(\omega\, t) \\ i\,\mathrm{Sin}\,(\omega\, t) \end{Bmatrix} K \sqrt{\frac{\varepsilon}{\mu}}\, e^{-\frac{G1\, \varepsilon_0\, \mu_0}{8\,\pi\, r}} = K \sqrt{\frac{\varepsilon}{\mu}}\, e^{-\frac{G1\, \varepsilon_0\, \mu_0}{8\,\pi\, r}}\, e^{i\,\omega\, t} \tag{23}$$

The Scalar function $\Psi[r,t]$ represents a fundamental solution of the Quantum Mechanical Schrödinger wave equation. [10]

4.1. Black Holes with Discrete Spherical Energy Levels at Sub-Atomic Dimensions

In order to effectively confine Electromagnetic Energy, a critical requirement is that the Poynting vector reaches a value of zero at the surface of the spherical confinement. Creating this confinement within a sphere necessitates the presence of a standing electromagnetic wave pattern, characterized by concentric spheres. Each of these spheres establishes an antinodal plane for either the Electric Field (E) or the Magnetic Field (B), with the radius distance between each sphere precisely equal to half the wavelength of the overall confinement.

Within this setup, a constant denoted as "k" is introduced, defined as $k = n\pi\lambda$, where "n" represents a natural number (1, 2, 3, 4,...) and λ signifies the wavelength of the radiation. This equation elucidates the structured connection between the wavelength, the constant k, and the natural number n within

the sphere of electromagnetic confinement in a spherical system.

4.2. Time and Radius Dependent Black Holes with Discrete Energy Levels, the Confinements of Electromagnetic Radiation Within Spherical Regions

Every concentric sphere represents an anti-nodal surface for the Electric Field (E) or the Magnetic Field (H). The Poynting Vector: $\bar{S} = \bar{E} \times \bar{H}$ at this spherical surface equals zero at any time and at any location at this sphere. The Electromagnetic Energy remains always within this sphere and the next concentric sphere. The concentric spheres have a difference in radius of one half wavelength of the electromagnetic radition within the confinement and a different discrete energy level. Every concentric sphere represents an anti-nodal suface of the electric field or the magnetic field [20].

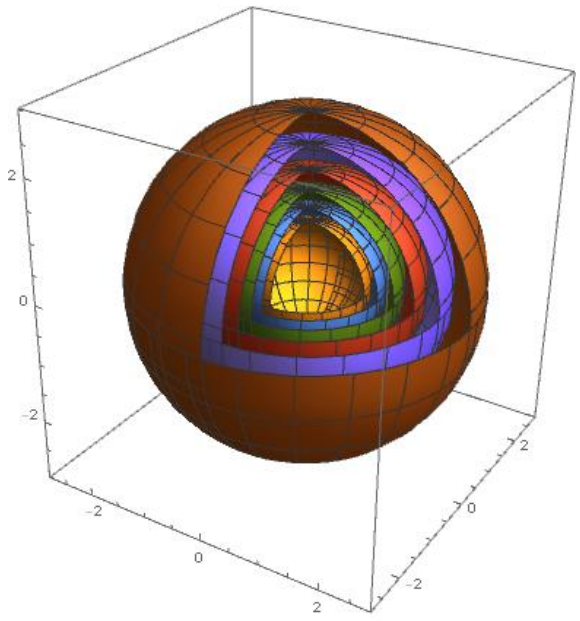

Figure 5. *Nodal and Antinodal Spheres for Standing (Confined) Spherical Electromagnetic waves with a 90 degrees phase shift between the Electric field and the Magnetic field. Equation (23).*

Figure 5 illustrates the spatial distribution of nodal and antinodal spheres concerning stationary, confined spherical electromagnetic waves characterized by a distinctive 90-degree phase disparity between the electric and magnetic fields. This configuration is delineated by Equation (23) which encapsulates the nuanced interplay between these fundamental electromagnetic components within a three-dimensional framework [20].

Figure 6 depicts the intricate nodal and anti-nodal spheres, emphasizing the scenario of standing, confined spherical electromagnetic waves where the wave number k is set at 3. Vegt Wim (Calculation 5, 16 March 2023) [19]. This visualization captures the unique 90-degree phase offset prevailing between the electric and magnetic fields. Equation (23) serves as the key mathematical representation encapsulating this phenomenon, further elucidating the interplay and characteristics of these electromagnetic waves within a specific spatial context.

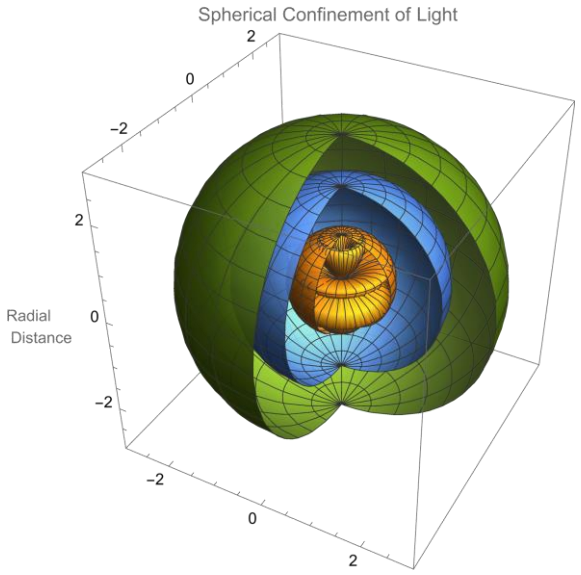

Figure 6. *Nodal- and Anti-nodal Spheres (k = 3) for Standing (Confined) Spherical Electromagnetic waves with a 90 degrees phase shift between the Electric field and the Magnetic field. Equation (23).*

Equation (24) describes a Time and Radius dependent BLACK HOLE.

$$\bar{E} = K\, e^{-\frac{G1\varepsilon 0\mu 0}{8\pi r}} \begin{pmatrix} 0 \\ \text{Sin[k r] Sin[}\omega\text{ t]} \\ \text{- Cos[k r] Cos[}\omega\text{ t]} \end{pmatrix}$$

$$\bar{H} = K\, e^{-\frac{G1\varepsilon 0\mu 0}{8\pi r}} \sqrt{\frac{\varepsilon_0}{\mu_0}} \begin{pmatrix} 0 \\ \text{Sin[k r] Cos[}\omega\text{ t]} \\ \text{- Cos[k r] Sin[}\omega\text{ t]} \end{pmatrix} \quad (24)$$

Equation (20) represents by the function Sin[k r] (k = 1,2,3,4….) the confinement of electromagnetic radiation between two concentric spheres. K represents the amplitude of the Electric/ Magnetic Field Intensty. [19]

4.3. Time and Polar Angle Dependent Black Holes

In the realm of time and polar angle-dependent black holes, Section 4.1.2 explores the intricate dynamics associated with

these celestial entities. Figure 7 offers a detailed insight into the nodal and antinodal regions across the polar angle, particularly emphasizing the case where the azimuthal quantum number m is defined as 3. Vegt Wim (Calculation 6, 23 April 2023) [20] These findings shed light on the behavior of standing, confined spherical electromagnetic waves featuring a distinct 90-degree phase discrepancy between the electric and magnetic fields, as encapsulated by Equation (25). [19]

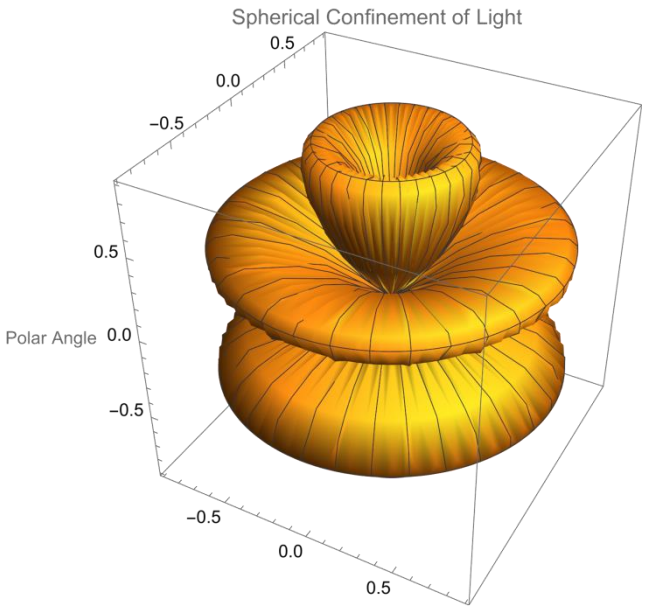

Figure 7. *Nodal- and Antinodal Polar Angle Regions (m = 3) for Standing (Confined) Spherical Electromagnetic waves with a 90 degrees phase shift between the Electric field and the Magnetic field. Equation (15).*

Equation (25) describes a Time and "Polar Angle" dependent BLACK HOLE Vegt Wim (Calculation 7, 15 May 2023) [21]:

$$\overline{E} = K\, e^{-\frac{G1\varepsilon 0\mu 0}{8\pi r}} \begin{pmatrix} 0 \\ \text{Sin}[m\ \theta]\ \text{Sin}[\omega\ t] \\ \text{Sin}[m\ \theta]\ \text{Cos}[\omega\ t] \end{pmatrix} \tag{25}$$

$$\overline{H} = K\, e^{-\frac{G1\epsilon 0\mu 0}{8\pi r}} \sqrt{\frac{\varepsilon_0}{\mu_0}} \begin{pmatrix} 0 \\ \text{Sin}[m\ \theta]\ \text{Cos}[\omega\ t] \\ -\text{Sin}[m\ \theta]\ \text{Sin}[\omega\ t] \end{pmatrix}$$

Equation (25) represents by the function $\text{Sin}[m\,\theta]$ (m = 1, 2, 3, 4…..) the confinement of electromagnetic radiation between two Polar Angular Regions [15].

Figure 8 illustrates the regions of nodal and antinodal behavior with respect to the polar angle, specifically focusing on cases where the azimuthal quantum number m is set to 3. This visualization pertains to standing, confined electromagnetic waves displaying a significant 90-degree phase differential between the electric and magnetic fields. The underlying dynamics are succinctly captured by Equation (15), providing a formal representation of these intriguing wave patterns.

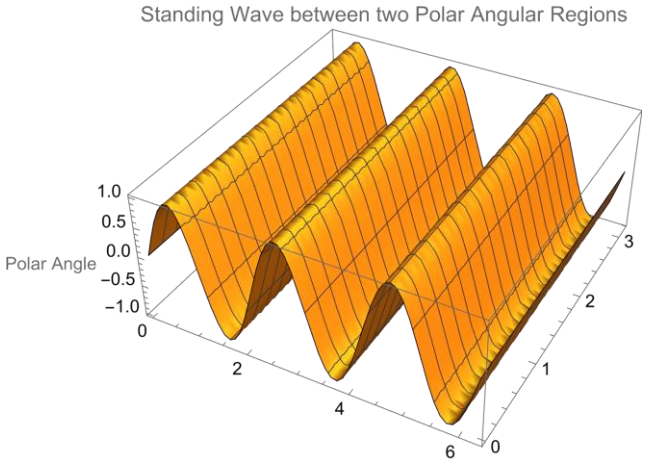

Figure 8. *Nodal- and Antinodal Polar Angle Regions (m = 3) for Standing (Confined) Electromagnetic waves with a 90 degrees phase shift between the Electric field and the Magnetic field. Equation (25).*

4.4. Time and Azimuthal Angular Dependent Black Holes

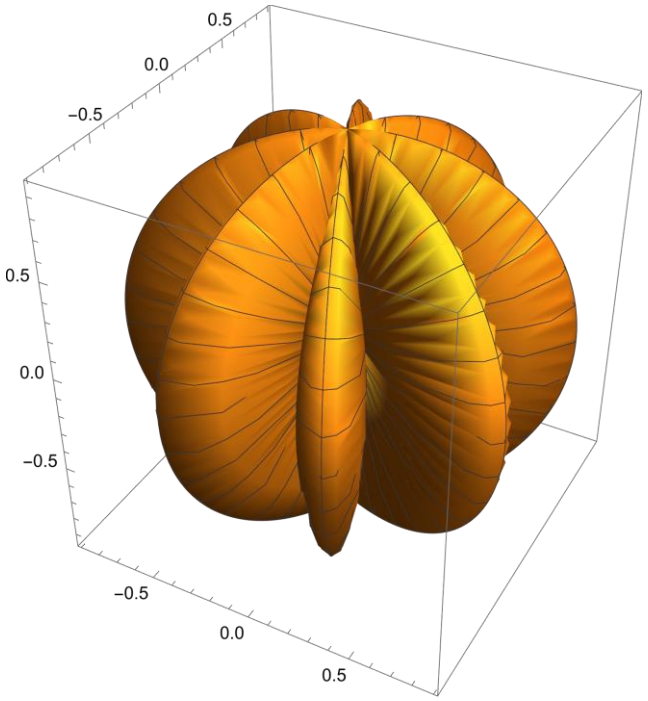

Figure 9. *Nodal- and Antinodal Azimuthal Angular Regions (n = 3) for Standing (Confined) Electromagnetic waves with a 90 degrees phase shift between the Electric field and the Magnetic field. Equation (26).*

Figure 9 Nodal- and Anti-nodal Azimuthal Angular Regions (n = 3) for Standing (Confined) Electromagnetic waves with a 90 degrees phase shift between the Electric field and the Magnetic field. Equation (26). Equation (26) describes a Time and "Polar Angle" dependent BLACK HOLE Vegt Wim (Calculation 7, 15 May 2023) [21]:

$$\overline{E} = K\, e^{-\frac{G1\varepsilon 0\mu 0}{8\pi r}} \begin{pmatrix} 0 \\ \text{Cos}[n\ \varphi]\ \text{Sin}[\omega\ t] \\ \text{Cos}[n\ \varphi]\ \text{Cos}[\omega\ t] \end{pmatrix}$$

$$\overline{H} = K\, e^{-\frac{G1\epsilon 0\mu 0}{8\pi r}} \sqrt{\frac{\varepsilon_0}{\mu_0}} \begin{pmatrix} 0 \\ \text{Cos}[n\ \varphi]\ \text{Cos}[\omega\ t] \\ -\text{Cos}[n\ \varphi]\ \text{Sin}[\omega\ t] \end{pmatrix} \quad (26)$$

The function denoted by Equation (26), where n ranges over integers (n = 1, 2, 3,...), encapsulates the confinement of electromagnetic radiation within two distinct Azimuthal Angular Regions, as referenced by [14, 15].

4.5. Time, Polar- and Azimuthal Angular Dependent Black Holes

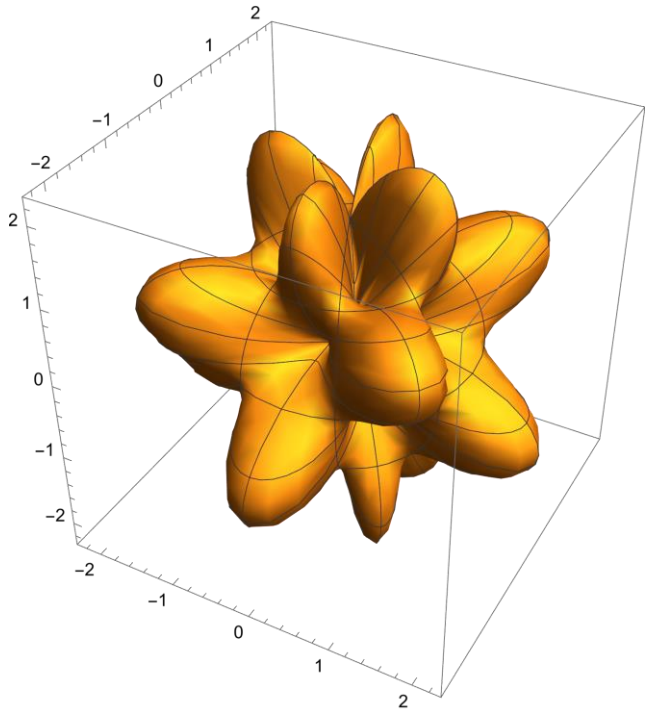

Figure 10. *Nodal- and Anti-nodal Polar Angular and Azimuthal Angular Regions (n = 4 and m = 4) for Standing (Confined) Electromagnetic waves with a 90 degrees phase shift between the Electric field and the Magnetic field. Equation (27).*

Figure 10 showcases the delineation of nodal and anti-nodal regions pertaining to both polar and azimuthal angular domains, specifically when n is set to 4 and m is set to 4. This visualization sheds light on the intricate behavior of standing, confined electromagnetic waves characterized by a distinct 90-degree phase difference between the electric and magnetic fields. The mathematical framework governing these phenomena is encapsulated by Equation (27), providing a formal expression of these electromagnetic wave patterns within the specified angular regions.

Equation (27) describes a Time "Azimuthal Angle" and "Polar Angle" dependent BLACK HOLE Vegt Wim (Calculation 7, 15 May 2023) [21]:

$$\overline{E} = K\, e^{-\frac{G1\varepsilon 0\mu 0}{8\pi r}} \begin{pmatrix} 0 \\ \text{Cos}[n\ \varphi]\ \text{Sin}[m\ \theta]\ \text{Sin}[\omega\ t] \\ \text{Cos}[n\ \varphi]\ \text{Sin}[m\ \theta]\ \text{Cos}[\omega\ t] \end{pmatrix}$$

$$\overline{H} = K\, e^{-\frac{G1\epsilon 0\mu 0}{8\pi r}} \sqrt{\frac{\varepsilon_0}{\mu_0}} \begin{pmatrix} 0 \\ -\text{Cos}[n\ \varphi]\ \text{Sin}[m\ \theta]\ \text{Cos}[\omega\ t] \\ \text{Cos}[n\ \varphi]\ \text{Sin}[m\ \theta]\ \text{Sin}[\omega\ t] \end{pmatrix} \quad (27)$$

Equation (27) represents by the function $\text{Cos}[n\ \varphi]$ (n = 1, 2, 3, 4…..) and $\text{Sin}[m\ \theta]$ (m = 1, 2, 3, 4…..) the confinement of electromagnetic radiation between two Azimuthal Angular Regions and two Polar Angulars Regions [14, 15].

4.6. Spherical Confinement of Light Beween Two Concentric Spheres Within Black Holess

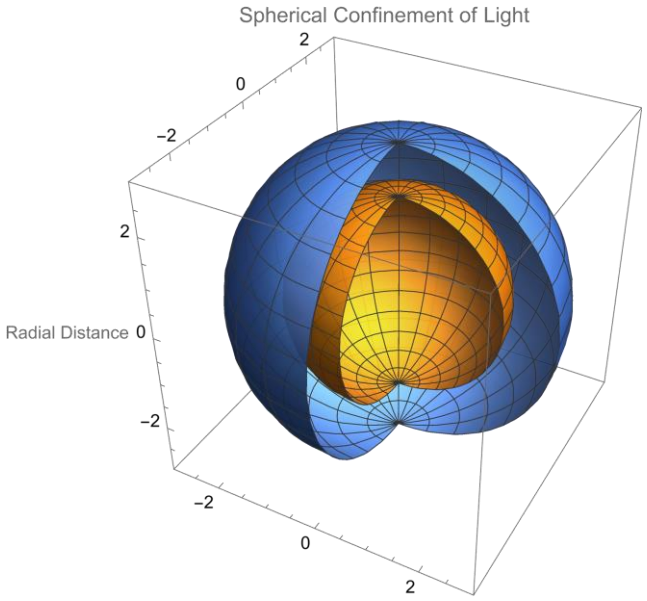

Figure 11. *Nodal- and Antinodal Regions for Standing (Confined) Electromagnetic waves with a 90 degrees phase shift between the Electric field and the Magnetic field. Equation (14).*

Figure 11 illustrates the nodal and antinodal regions associated with standing, confined electromagnetic waves featuring a 90-degree phase differential between the electric and magnetic fields. The intricacies of this wave behavior are represented mathematically by Equation (14), offering a formal description of the electromagnetic field dynamics within this context.

Equation (28) captures the phenomenon of the reflection of Confined Electromagnetic Energy within the confines of a Black Hole, delineated between two concentric spheres. In this scenario, the speed of light, which is contingent upon the variable "r" representing the radial distance, undergoes a change in direction commensurate with the frequency of the confined light, or Electromagnetic Radiation.

Remarkably, a Black Hole possesses the capacity to undergo a process of splitting into two distinct Black Holes characterized by differing radii. During this transformation, the original Black Hole transitions to a lower energy level, akin to an atom descending to a lower energy state. The resultant new Black Holes formed as a consequence of this splitting represent the disparity in energy levels, resembling the analogous behavior of an atom transitioning between energy levels within its atomic structure. Vegt Wim (Calculation 5, 16 March 2023) [19]:

$$\bar{E} = K\, e^{-\frac{G1\varepsilon 0\mu 0}{8\pi r}} f\left[t - \frac{\sqrt{\varepsilon_0\ \mu_0}\ \text{Cos}[2\ k\ r]}{2\ k}\right] \begin{pmatrix} 0 \\ \text{Sin}[k\ r]\ \text{Sin}[\omega\ t] \\ -\text{Cos}[k\ r]\ \text{Cos}[\omega\ t] \end{pmatrix}$$

$$\bar{H} = K\, e^{-\frac{G1\epsilon 0\mu 0}{8\pi r}} f\left[t - \frac{\sqrt{\varepsilon_0\ \mu_0}\ \text{Cos}[2\ k\ r]}{2\ k}\right] \sqrt{\frac{\varepsilon_0}{\mu_0}} \begin{pmatrix} 0 \\ -\text{Sin}[k\ r]\ \text{Cos}[\omega\ t] \\ -\text{Cos}[k\ r]\ \ \text{Sin}[\omega\ t] \end{pmatrix} \tag{28}$$

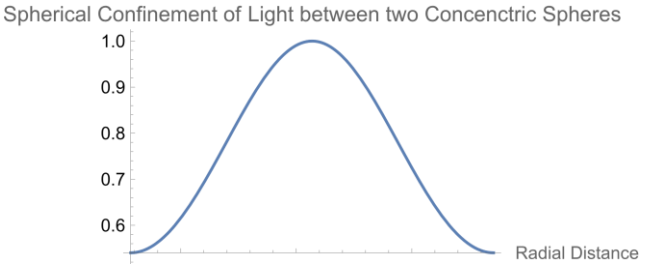

Figure 12. *Nodal- and Antinodal Regions for Standing (Confined) Electromagnetic within two concentric spheres. Equation (18).*

Figure 12 presents a visual representation of the nodal and anti-nodal regions characterizing standing, confined electromagnetic waves enclosed within two concentric spheres. The electromagnetic field behaviors within this configuration are mathematically defined by Equation (18), offering a precise formulation of the wave dynamics within the specified spatial constraints.

4.7. Universal Equilibrium in the "Concept of Quantum Mechanical Probability" in "The New Theory"

The 4-dimensional notation for the divergence of the Stress-Energy Tensor (25) expresses in the 4th dimension (time dimension) the law of Conservation of Energy". For an Electromagnetic Field the law for conservation of Energy has been expressed as:

$$\bar{f}^4 = \begin{pmatrix} f_4 \\ f_3 \\ f_2 \\ f_1 \end{pmatrix} = \square \bullet \bar{\bar{T}} = \begin{pmatrix} \nabla \cdot \bar{S} + \frac{\partial\, w}{\partial\, t} \\ f_3 \\ f_2 \\ f_1 \end{pmatrix} = \bar{0}^4 \tag{29}$$

From the equation for the "Conservation of Electromagnetic Energy" (38.1) the "Fundamental Equation for Confined Electromagnetic Interaction" in "The New Theory" will be derived, which equals the Relativistic Quantum Mechanical "Dirac" equation and the Schrödinger wave equation at velocities relative low compared to the speed of light.

The "Fundamental Equation for Confined Electromagnetic Interaction" in "The Proposed Theory" can be considered to be the relativistic version of the Quantum Mechanical Schrödinger wave equation, which equals the Quantum Mechanical Dirac Equation.

5. Confined Electromagnetic Energy Within a 4-dimensional Equilibrium

The physical concept of quantum mechanical probability waves has been created during the famous 1927 5th Solvay Conference. During that period there were several circumstances which came just together and made it possible to create a unique idea of "Material Waves" (Solutions of Schrödinger's wave equation) being complex (partly real and partly imaginary) and describing the probability of the appearance of a physical object (elementary particle) generally

indicated as "Quantum Mechanical Probability Waves".

The idea of complex (probability) waves is directly related to the concept of confined (standing) waves. Characteristic for any standing acoustical wave is the fact that the Velocity and the Pressure (Electric Field and Magnetic Field in QLT) are always shifted over 90 degrees. The same principle does exist for the standing (confined) electromagnetic waves,

For that reason every confined (standing) Electromagnetic wave can be described by a complex sum vector $\bar{\phi}$ of the Electric Field Vector $\bar{E}$ and the Magnetic Field Vector $\bar{B}$ ($\bar{E}$ has 90 degrees phase shift compared to $\bar{B}$).

The vector functions $\bar{\phi}$ and the complex conjugated vector function $\bar{\phi}^*$ will be written as:

$$\bar{\phi} = \frac{1}{\sqrt{2\,\mu}}\left(\bar{B} + i\,\frac{\bar{E}}{c}\right) \tag{30}$$

$\bar{B}$ equals the magnetic induction, $\bar{E}$ the electric field intensity ($\bar{E}$ has + 90 degrees phase shift compared to $\bar{B}$) and c the speed of light.

The complex conjugated vector function $\bar{\phi}^*$ equals:

$$\bar{\phi}^* = \frac{1}{\sqrt{2\,\mu}}\left(\bar{B} - i\,\frac{\bar{E}}{c}\right) \tag{31}$$

The dot product equals the electromagnetic energy density w:

$$\bar{\phi}\,.\,\bar{\phi}^* = \frac{1}{2\,\mu}\left(\bar{B} + i\,\frac{\bar{E}}{c}\right).\left(\bar{B} - i\,\frac{\bar{E}}{c}\right) = \frac{1}{2}\,\mu\,H^2 + \frac{1}{2}\,\varepsilon\,E^2 = w \tag{32}$$

Using Einstein's equation $W = m\,c^2$, the dot product equals the electromagnetic mass density w:

$$\bar{\phi}\,.\,\bar{\phi}^*\frac{1}{c^2} = \frac{\varepsilon}{2}\left(\bar{B} + i\,\frac{\bar{E}}{c}\right).\left(\bar{B} - i\,\frac{\bar{E}}{c}\right) = \frac{1}{2}\varepsilon\,\mu^2H^2 + \frac{1}{2}\varepsilon^2E^2 = \rho\ [kg/m^3] \tag{33}$$

The cross product is proportional to the Poynting vector: Vegt Wim (1995) [10].

$$\bar{\phi} \times \bar{\phi}^* = \frac{1}{2\,\mu}\left(\bar{B} + i\,\frac{\bar{E}}{c}\right) \times \left(\bar{B} - i\,\frac{\bar{E}}{c}\right) = i\sqrt{\varepsilon\,\mu}\ \ \bar{E} \times \bar{H} = i\sqrt{\varepsilon\,\mu}\ \bar{S} \tag{34}$$

This article presents a new "Gravitational-Electromagnetic Equation" describing Electromagnetic Field Configurations which are simultaneously the Mathematical Solutions for the Scalar Quantum Mechanical "Schrodinger Wave Equation" and more exactly the Mathematical Solutions for the Tensor representation of the "Relativistic Quantum Mechanical Dirac Equation" (41). [19]

The 4-dimensional divergence of the sum of the Electromagnetic Stress-Energy tensor expresses the 4-dimensional Force-Density vector (expressed in $[N/m^3]$ in the 3 spatial coordinates) as the result of Electro-Magnetic-Gravitational interaction.

$$f^{\mu} = \partial_{\nu}\,T^{\mu\nu} = 0 \tag{35}$$

In vector notation the 4-dimensional Force-Density vector can be written as:

$$\bar{f}^4 = \begin{pmatrix} f_4 \\ f_3 \\ f_2 \\ f_1 \end{pmatrix} = \square \bullet \bar{\bar{T}} = 0 \tag{36}$$

The fundamental boundary condition for this alternative approach to gravity is the requirement that the Force 4 vector equals zero in the 4 dimensions, expressing a universal 4-dimensional equilibrium:

The 3 spatial components of the Force-Density vector, as a result of Electro-Magnetic-Gravitational interaction can be written as:

Substituting the electromagnetic values for the electric field intensity "E" and the magnetic field intensity "H" in (36) results in the 4-dimensional representation of the Electro-Magnetic-Gravitational Fields Equation (37):

Energy-Time Domain

$$\left(f_4\right) \quad \Leftrightarrow \quad \nabla \cdot \left(\bar{E} \times \bar{H}\right) + \frac{1}{2} \frac{\partial\left(\varepsilon_0 \left(\bar{E} \cdot \bar{E}\right) + \mu_0 \left(\bar{H} \cdot \bar{H}\right)\right)}{\partial t} = 0$$

3-Dimensional Space Domain

$$\begin{pmatrix} f_3 \\ f_2 \\ f_1 \end{pmatrix} \quad \Leftrightarrow \quad -\frac{1}{c^2}\frac{\partial\left(\bar{E} \times \bar{H}\right)}{\partial t} + \varepsilon_0 \bar{E}\left(\nabla \cdot \bar{E}\right) - \varepsilon_0 \bar{E} \times \left(\nabla \times \bar{E}\right) + \mu_0 \bar{H}\left(\nabla \cdot \bar{H}\right) - \mu_0 \bar{H} \times \left(\nabla \times \bar{H}\right) = \bar{0} \tag{37}$$

In which f_1, f_2, f_3, represent the force densities in the 3 spatial dimensions and f_4 represent the force density (energy flow) in the time dimension (4th dimension). Equation (37) can be written as:

Energy-Time Domain

Conservation of Energy

B-7

$$\left(f_4\right) \quad \nabla \cdot \bar{S} + \frac{\partial w}{\partial t} = 0 \tag{38.1}$$

3-Dimensional Space Domain

B-1 B-2 B-3

B-4 B-5

$$\begin{pmatrix} f_3 \\ f_2 \\ f_1 \end{pmatrix} \quad -\frac{1}{c^2}\frac{\partial\left(\bar{E} \times \bar{H}\right)}{\partial t} + \varepsilon_0 \bar{E}\left(\nabla \cdot \bar{E}\right) - \varepsilon_0 \bar{E} \times \left(\nabla \times \bar{E}\right) + \mu_0 \bar{H}\left(\nabla \cdot \bar{H}\right) - \mu_0 \bar{H} \times \left(\nabla \times \bar{H}\right) = \bar{0} \tag{38.2}$$

The 4th term in equation (38.1) can be written in the terms of the Poynting vector "S" and the energy density "w" representing the electromagnetic law for the conservation of energy (Newton's second law of motion).

6. The 4-dimensional Relativistic Dirac Equation

Substituting (32) and (34) in Equation (38.1) results in The 4-Dimensional Tensor presentation for the relativistic quantum mechanical Dirac Equation (39):

$$\left(x_4\right) \quad \nabla \cdot \left(\bar{\phi} \times \overline{\phi^*}\right) + \frac{i}{c}\frac{\partial \bar{\phi} \cdot \bar{\phi}^*}{\partial t} = 0$$

$$\begin{pmatrix} x_3 \\ x_2 \\ x_1 \end{pmatrix} \quad \frac{i}{c}\frac{\partial\left(\bar{\phi} \times \overline{\phi^*}\right)}{\partial t} - \left(\bar{\phi} \times \left(\nabla \times \overline{\phi^*}\right) + \overline{\phi^*} \times \left(\nabla \times \bar{\phi}\right)\right) + \left(\bar{\phi}\left(\nabla \cdot \overline{\phi^*}\right) + \overline{\phi^*}\left(\nabla \cdot \bar{\phi}\right)\right) = 0 \tag{39}$$

To transform the electromagnetic vector wave function $\bar{\phi}$ into a scalar (spinor or one-dimensional matrix representation), the Pauli spin matrices σ and the following matrices (Ref. 3 page 213, equation 99) are introduced:

$$\bar{\alpha} = \begin{bmatrix} 0 & \sigma \\ \sigma & 0 \end{bmatrix} \quad \text{and} \quad \bar{\beta} = \begin{bmatrix} \delta_{ab} & 0 \\ 0 & -\delta_{ab} \end{bmatrix} \tag{40}$$

The Equations (6), (32) and (34) can be written in tensor presentation as the 4-Dimensional Relativistic Quantum Mechanical Dirac Equation: [9] (Equation 102, page 213)

$$(x_4) \qquad \left(\frac{i\, m\, c}{h} \bar{\beta} + \bar{\alpha} \,.\, \nabla \right) \psi = - \frac{1}{c} \frac{\partial \psi}{\partial t} \tag{41.1}$$

$$\begin{pmatrix} x_3 \\ x_2 \\ x_1 \end{pmatrix} \qquad - \frac{1}{c^2} \frac{\partial (\bar{E} \times \bar{H})}{\partial t} + \varepsilon_0 \bar{E} (\nabla \,.\, \bar{E}) - \varepsilon_0 \bar{E} \times (\nabla \times \bar{E}) + \tag{41}$$

$$+ \mu_0 \bar{H} (\nabla \,.\, \bar{H}) - \mu_0 \bar{H} \times (\nabla \times \bar{H}) + \gamma_0 \bar{g} (\nabla \,.\, \bar{g}) - \gamma_0 \bar{g} \times (\nabla \times \bar{g}) = \bar{0} \tag{41.2}$$

7. The Fundamental Experiment to Validate the New Theory in Physics

The fundamental foundation for Einstein's Theory of General Relativity is the "Curvature of Space and Time" due to a Gravitational Field. In the "Theory of General Relativity" Gravitational RedShift has been explained by a change in time and space resulting is a change in the observed frequency shift in the spectrum of the light being emitted by far away Galaxies. The foundation for Einstein's theory of General Relativity is a constant value for the speed of light in the absence of a gravitational field Daniel Y. Gerazi (2010) [1].

In the "New Theory" the fundamental foundation is "Equilibrium". Equilibrium for the "5 fundamental force densities in light" in any direction at any time and at any location. The 5 fundamental forces in light are:

1) "Inertia Force" (Energy has always inertia according Einstein's $E = m\, c^2$)

2) "Electric Force"

3) "Magnetic Force"

4) "Electric Force" due to the "Lorentz Transformation" of the "Magnetic Force"

5) "Magnetic Force" due to the "Lorentz Transformation" of the "Electric Force"

The speed of light has been fully controlled by the perfect equilibrium between the 5 fundamental force densities in any direction at any time and at any location. For a single beam of light the perfect equilibrium between the 5 fundamental forces always results in the speed of light:

$$c = \frac{1}{\sqrt{\varepsilon_0\, \mu_0}} \tag{42}$$

However in this experiment 3 beams of light with the same frequency and the same phase and 3 controllable (LPA) different intensities K1, K2 and K3 will cross each other in 3 orthogonal directions. This will result in different boundary conditions for the total electromagnetic radiation and will be measurable by a changing in the speed of light. In this experiment by a changing of the speed of light in the chosen z-direction. The changing of the speed of light will become visible by a change in the interference patterns of the 2 LASER beams. The original beam and the manipulated beam.

The solution for equation (8) has been calculated in Mathematica when 3 laser beams cross each other perpendicular and will cause a change in the speed of light within the intersection of the 3 crossing Laser Beams due to Electromagnetic Interaction. According the calculations in Mathematica 11.3 at the exact "location dependent speed of light c(x,y,z)" there will be a perfect equilibrium between all the electromagnetic- inertia- and radiation pressure force densities at any time in any direction:

$$\frac{1}{c(x,y,z)} = \frac{\left(K_2^2\, x - K_1 K_3\, x + K_3^2\, y + K_1^2\, z - K_2 \left(K_1\, y + K_3\, z \right) \right) \sqrt{\varepsilon_0} \sqrt{\mu_0}}{K_1^2 + K_2^2 + K_3^2} \tag{43}$$

The findings articulated in equation (43) have been documented in Vegt Wim, Calculation 8 (16 June 2024). The alteration in the velocity of light within the designated cross-sectional area will manifest in the interference patterns observed on Screen 1 and Screen 2. This phenomenon can be elicited by modulating the intensity of the secondary and tertiary LASER beams using the two "LASER Power Attenuators" (as denoted in blue) subsequent to the bifurcation of the beam(s) through the beamsplitter(s).

From the implications of equation (43), it can be concluded that only within the intersection of the three distinct LASER beams does the resultant electromagnetic wave propagate as a singular entity. [22]

This unified electromagnetic wave is characterized by a

single Poynting vector, which corresponds to the vectorial summation of the Poynting vectors associated with the three individual LASER beams. This phenomenon underpins the principle that the total momentum of the resultant electromagnetic wave is equivalent to the cumulative momentum derived from the three separate LASER beams, a consequence of electromagnetic interaction. [24]

The interaction patterns among the three corresponding LASER beams will become evident within regions defined by dimensions that correspond to the wavelengths of the original LASER beam. Consequently, the observation of these specific interaction patterns necessitates the use of a high-resolution camera equipped with a macro-zoom lens.

Technical Setup for the Experiment to demonstrate that the speed of light will change in the area of Electromagnetic Interaction.

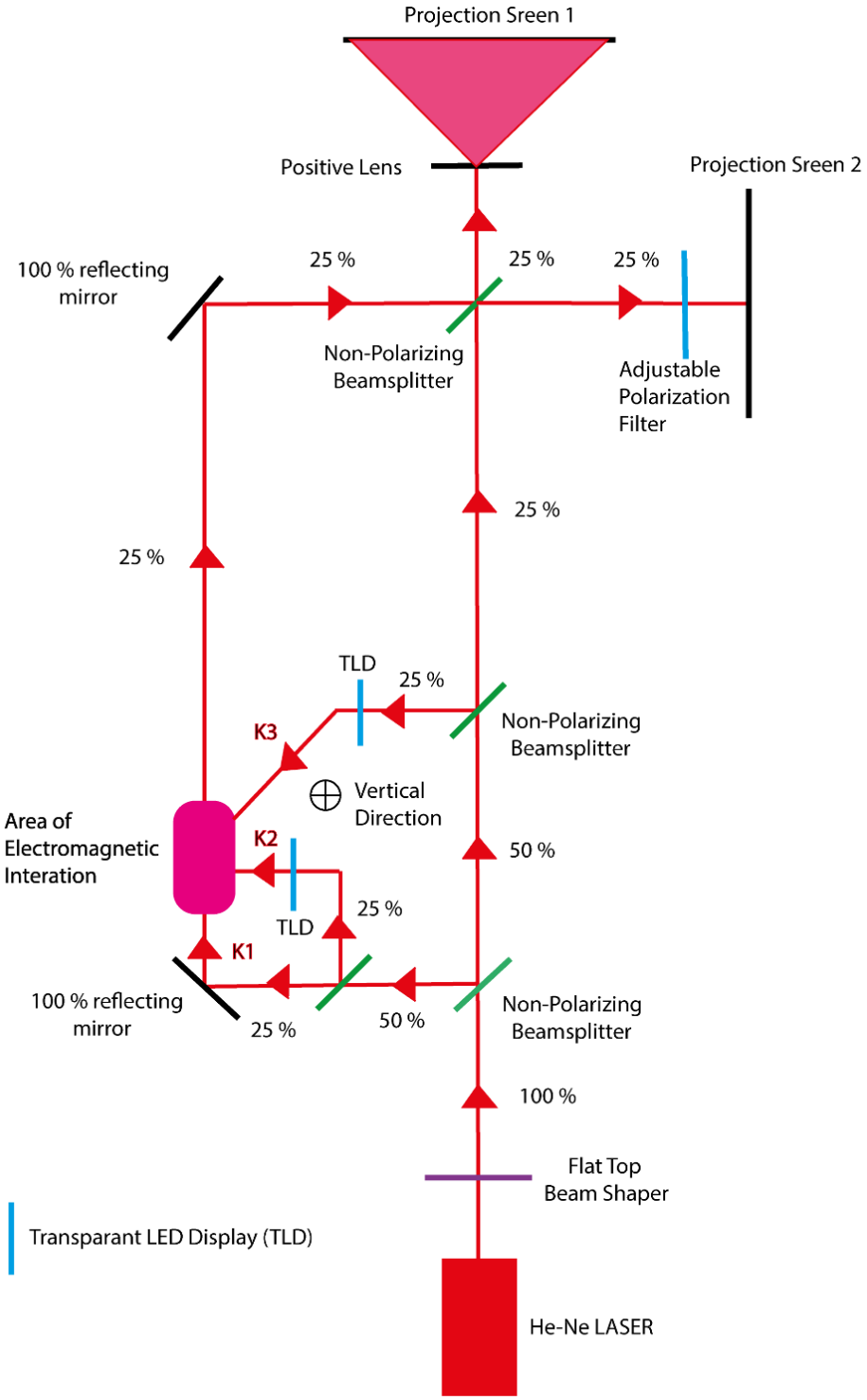

Figure 13. *Arrangement for Demonstrating "Electromagnetic Interaction" involving three orthogonal coherent laser beams interacting within a confined cross-sectional area to exhibit "Electromagnetic Interaction".*

8. Summary and Conclusions

In conclusion, this study provides a meticulous examination of the intricate interactions among black holes, dark matter, and the fundamental forces of light, gravity, and electromagnetism within a ten-dimensional hyperspace, thereby establishing a transformative paradigm for astrophysics and astronomy. By introducing the concept of "Equilibrium" and scrutinizing the constancy of the speed of light under specific conditions, the research reconfigures our comprehension of these cosmic phenomena. The integration of the Stress-Energy Tensor with the Gravitational Tensor offers an innovative tensor framework applicable to phenomena such as black holes, enhancing our understanding of gravitational and electromagnetic interactions beyond the confines of General Relativity.

Furthermore, this investigation elucidates the possibility that light may undergo implosion due to its intrinsic gravitational field, resulting in "GEONs" exhibiting properties analogous to elementary particles. This assertion challenges the invariance of light speed and underscores the relevance of the "Equilibrium" concept. Through the synthesis of the Stress-Energy Tensor and the Gravitational Tensor, the study deepens insights into black holes and the gravitational-electromagnetic interplay, thereby questioning the established principles of General Relativity.

This theoretical construct aspires to bridge the gap between Quantum Physics and General Relativity, supported by empirical data derived from Galileo satellites and MASER frequency measurements. Ultimately, the findings of this research signify significant advancements in our understanding of the cosmos and present profound implications for future investigation at the intersection of classical and quantum physics.

Abbreviations

GEON	Gravitational Electromagnetic Entity
LASER	Light Amplification by Stimulated Emission Radiation
MASER	Microwave Amplification by Stimulated Emission Radiation
QLT	Quantum Light Theory

Author Contributions

Wim Vegt is the sole author. The author read and approved the final manuscript.

Data Availability Statement

All Data and Calculations have been published at: https://quantumlight.science/

Conflicts of Interest

The author declares no conflicts of interest.

References

[1] Daniel Y. Gerazie; Lunar Laser Ranging Test of the Invariance of c; NASA/Goddard Space Flight Center, Laboratory for ExoPlanets and Stellar Astrophysics, Code 667, Greenbelt, MD 20771; https://arxiv.org/pdf/0912.3934

[2] Delva P, Puchades N, Schönemann E, Dilssner F, Courde C et. al 4 December 2018, Gravitational Redshift Test Using Eccentric Galileo Satellites, Phys. Rev. Lett. 121, 231101 – Published; https://doi.org/10.1103/PhysRevLett.121.231101

[3] Einstein Albert 1953, On the Influence of Gravitation on the Propagation of Light; Annalen der Physik (ser. 4), 35, 898–908, http://myweb.rz.uni-augsburg.de/~eckern/adp/history/einstein-papers/1911_35_898-908.pdf

[4] Einstein Albert (originally published in 1953) 19 Jul 2011, "Elementare Uberlegungen zur Interpretation der Grundlagen der Quanten-Mechanik", (Oliver and Boyd), pages 33-40; Translated into English, 2011, https://doi.org/10.48550/arXiv.1107.3701

[5] Herrmann Sven, Felix Finke, Martin Lülf, Olga et. al 4 December 2018, Gravitational Redshift Test Using Eccentric Galileo Satellites, Phys. Rev. Lett. 121, 231102, https://doi.org/10.1103/PhysRevLett.121.231102

[6] Maxwell James Clerk 01 January 1865, A dynamical theory of the electromagnetic field; https://royalsocietypublishing.org/doi/10.1098/rstl.1865.0008

[7] Nikko John Leo S. Lobos, Reggie C. Pantig; Generalized Extended Uncertainty Principle Black Holes: Shadow and lensing in the macro- and microscopic realms; Physics 2022, 4(4), 1318-1330; https://doi.org/10.3390/physics4040084

[8] Raymond J. Beach; A classical Field Theory of Gravity and Electromagnetism; Journal of Modern Physics; 2014, 5, 928-939; https://doi.org/10.4236/jmp.2014.510096

[9] Vegt Wim; A Continuous Model of Matter based on AEONs, Physics Essays, Volume 8, Number 2, 1995; Equation 15 Page 202.

[10] Vegt Wim; A Continuous Model of Matter based on AEONs, Physics Essays, Volume 8, Number 2, 1995; Equation 119 Page 216, Equation A45 Page 221 and Equation A46 Page 221.

[11] Vegt Wim 2002; The Maxwell-Schrödinger-Dirac Correspondence in Auto Confined Electromagnetic Fields; Equation 3 Page 3; Annales Fondation Louis de Broglie, Volume 27, no 1. https://fondationlouisdebroglie.org/AFLB-271/aflb271p001.pdf

[12] Vegt Wim 2 October 2021; The 4-Dimensional Dirac Equation in Relativistic Field Theory; European Journal of Applied Sciences; Equation 23 Page 49; https://doi.org/10.14738/aivp.91.9403

[13] Vegt Wim; "The Origin of Gravity in "Quantum Light Theory"; OSF Preprints; 14 October 2022; https://doi.org/10.31219/osf.io/n43yd

[14] Vegt Wim; The Origin of Gravity; Research & Reviews: Journal of Pure and Applied Physics; Manuscript No. JPAP-22-76022 (A); Equation 21 Page 13; Published: 26-Oct-2022; https://www.rroij.com/peer-reviewed/the-origin-of-gravity-91966.html

[15] Vegt Wim; The speed of light by Electromagnetic Interaction; Calculation 1; 21 June 2022; https://community.wolfram.com/groups/-/m/t/2576692?p_p_auth=mTldHX3v

[16] Vegt Wim; Gravitational RedShift between two Atomic Clocks, Calculation 2; 16 July 2023; https://community.wolfram.com/groups/-/m/t/2622560?p_p_auth=EC8QO0Xz

[17] Vegt Wim; Propagation of Light within a Gravitational Field in Quantum Light Theory, Calculation 3; 25 August 2022; https://community.wolfram.com/groups/-/m/t/2576537

[18] Vegt Wim; Black Holes with Discrete Spherical Energy Levels, Calculation 4; 21 February 2023; https://community.wolfram.com/groups/-/m/t/2896941?p_p_auth=D7ZKuo3k

[19] Vegt Wim; Time and Radius dependent GEONs with discrete Energy Levels, Calculation 5; 16 March 2023; https://community.wolfram.com/groups/-/m/t/2991686?p_p_auth=CGtF3Tkg

[20] Vegt Wim; Time and Polar Angular Regions dependent GEONs with discrete energy levels, Calculation 6; 23 April 2023; https://community.wolfram.com/groups/-/m/t/2901457?p_p_auth=H4jjDHmQ

[21] Vegt Wim; Time and Azimuthal Regions dependent GEONs with discrete energy levels, Calculation 7; 15 May 2023; https://community.wolfram.com/groups/-/m/t/3200586?p_p_auth=TWz8jyxO

[22] Vegt Wim; An Experiment to test General Relativity: Changing the speed of light by Electromagnetic Interaction, Calculation 8; 16 June 2024.

[23] Vegt Wim; A Perfect Equilibrium inside a Black Hole, Calculation 9; Wolfram Community: https://community.wolfram.com/groups/-/m/t/3087823?p_p_auth=dpH7iBMg

[24] Vegt Wim; An Experiment to test General Relativity: Changing the speed of light by Electromagnetic Interaction; Calculation 10.

[25] Weng Zihua, Influence of velocity curl on conservation laws, October 2008, https://doi.org/10.48550/arXiv.0810.0065

[26] Wheeler John Archibald; GEONs, Physical Review Journals Archive, 97, 511, Issue 2, pages 511-526, Published 15 January 1955, Publisher: American Physical Scociety, https://doi.org/10.1103/PhysRev.97.511

[27] Joshua N. Benabou, Quentin Bonnefoy, Malte Buschmann, Soubhik Kumar, and Benjamin R. Safdi; Cosmological dynamics of string theory axion strings; Phys. Rev. D 110, 035021 – Published 19 August 2024; https://doi.org/10.1103/PhysRevD.110.035021

[28] Astrid Eichhorn, Rafael R. Lino dos Santos, and Jo ão Lucas Miqueleto; From quantum gravity to gravitational waves through cosmic strings; Phys. Rev. D 109, 026013, 30 January 2024; https://doi.org/10.1103/PhysRevD.109.026013

[29] N. Mavromatos, P. Dorlis and S. N. Vlachos; Torsion-induced axions in string theory, quantum gravity and the cosmological tensions; Proceedings of Science, Volume 463, Workshop on the Standard Model and beyond, 2023; https://doi.org/10.22323/1.463.0162